decline in the MH_2^+ cross section is competition with another process. The peaks in these cross sections correlate well with the onset of MH^+ production, about 2 eV for Sc^+, Y^+, and La^+ and 2.5 eV for Lu^+. This observation can be taken as evidence that MH^+ and MH_2^+ are formed via a common intermediate, II. Since MH^+ formation is a bond fission while MH_2^+ production requires a rearrangement, formation of MH^+ could rapidly deplete the population of intermediate II even though it is the more endothermic pathway.

Summary

The reaction of Sc^+, Y^+, La^+, and Lu^+ with methane results in MCH_2^+ at low energy, with MH^+ and a small amount of MCH_3^+ formed at higher energies. With ethane, $MC_2H_4^+$ and $MC_2H_2^+$ are formed exothermically for M = Sc, Y, and La and endothermically for M = Lu. Endothermic channels for all four ions include MH_2^+ at low energies and MH^+, MCH_3^+, and MCH_2^+ at elevated energies. The thermochemistry of these various product ions is derived from analysis of the reaction thresholds. The bond energies (given in Table V) indicate single bonds to H and CH_3 and double bonds to CH_2. The values are generally consistent with an "intrinsic bond energy" model corrected for the electronic excitation needed for promotion to an orbital suitable for bonding.

The experimental results of both systems are interpreted to indicate that most of the reactivity is due to an insertive mechanism but that, with methane, some fraction of the MH^+ is due to a more direct process. The amount of insertive reaction relative to direct reaction increases down the third column from Sc^+ to Y^+ to La^+, with Lu^+ being more direct than the other elements. Qualitative molecular orbital arguments previously shown to be useful in describing the reaction of metal ions with H_2 and CH_4 are consistent with the results seen. There is an apparent bottleneck in the pathway to reach the ground-state insertion products H-M^+-CH_3 and H-M^+-C_2H_5 for the most highly populated states of Sc^+, Y^+, and La^+. This is attributed to a surface crossing between the triplet surfaces of the reactants and the singlet surfaces of the intermediates.

Consistent with earlier results for Sc^+ with ethane, Y^+ and apparently La^+ dehydrogenate ethane by two mechanisms: 1,2-dehydrogenation to form M^+-ethane at low energy and 1,1-dehydrogenation to form the metal-ethylidene ion at higher energy. There are also two channels for double dehydrogenation of ethane by Sc^+, Y^+, and La^+. The data for all three elements are similar and are consistent with either of two mechanisms: one involving different electronic states of the intermediates formed and one where vibrationally excited H_2 is eliminated. For Lu^+ there is only one apparent channel for both reactions.

Overall, the reactivities of the group 3 metal ions with methane and ethane are quite similar. Futher, the thermochemistry of the metal hydride ions, metal dihydride ions, metal methyl ions, and metal methylidene ions for Sc^+, Y^+, and La^+ are all comparable. Lu^+ differs somewhat in both respects. The difference between La^+ (which has no 4f electrons) and Lu^+ (which has a filled 4f shell) must be a result of the differing 4f orbital occupancy. However, there is no indication of direct participation of the 4f orbitals. Rather the effect of the 4f orbitals is probably an indirect one. Namely, the occupation of these orbitals raises the energy of the 5d shell such that the two valence electrons in the ground state of Lu^+ both occupy the 6s orbital. In La^+, the energy of the 5d and 6s orbitals is much closer, leading to open shell electron configurations. The closed-shell stability of the $Lu^+(^1S,6s^2)$ ground state probably accounts for its distinct reactivity compared with Sc^+, Y^+, and La^+.

Acknowledgment. This research is funded by National Science Foundation Grant No. 8796289. L.S.S. thanks the NSF for a predoctoral fellowship.

High-Resolution Absorption and Luminescence Spectroscopy of a Cyclometalated Rhodium(III) Complex: $[Rh(phpy)_2(bpy)]^+$

Arne Zilian, Urs Maeder,† Alex von Zelewski,† and Hans U. Güdel*

Contribution from the Institut für Anorganische und Physikalische Chemie, Universität Bern, Freiestrasse 3, 3000 Bern 9, Switzerland. *Received October 31, 1988*

Abstract: The title complex was prepared in crystalline form as the Cl^- and PF_6^- salt and studied by absorption and luminescence spectroscopy down to 5 K. The highly resolved crystal spectra of the PF_6^- salt allow the location of four electronic origins for the lowest energy transitions: 22 030 (A), 22 078 (B), 22 128 (C), and 22 150 cm^{-1} (D). The rich fine structure in the absorption spectrum between 22 000 and 26 000 cm^{-1} is fully interpreted as vibrational sideband structure on the origins C and D. The sharp structure of the low-temperature luminescence spectrum, which is built on the origin A, is distinctly different. In terms of the usual classification, the transitions C and D are assigned as singlet-triplet (RhLCT) charge-transfer transitions. The transitions A and B, exhibiting some properties typical of ligand-centered singlet-triplet excitations but also some significant deviations, are more difficult to classify.

1. Introduction

The study of the lowest energy excited states in chelate complexes of $4d^6$ and $5d^6$ metal ions continues to attract a great deal of attention. Complexes with a broad range of photophysical and photochemical properties have been synthesized by chemical variation of the ligands and the metal ion.[1-3] Measurements of absorption and luminescence spectra in solutions and glasses at room and liquid-nitrogen temperature are usually combined with a study of the quantum yield and decay behavior of luminescence to characterize new complexes.

Inhomogeneous broadening of absorption and emission lines in glassy matrices is often very pronounced, thus seriously reducing their information content. Nonexponential luminescence decay behavior originating from a distribution of different sites in the sample is frequently observed in such environments. Many glasses have properties depending on their history, which seriously limits

* Author to whom correspondence is addressed.
† Institut de Chimie Minérale, Université de Fribourg Pérolles, 1700 Fribourg, Switzerland.

(1) Krausz, E. R.; Ferguson, J. *Prog. Inorg. Chem.*, in press.
(2) Juris, A.; Barigeletti, F.; Campagna, S.; Balzani, V.; Belser, P.; von Zelewsky, A. *Coord. Chem. Rev.* **1988**, *84*, 85.
(3) Lees, A. J. *Chem. Rev.* **1987**, *87*, 711.

0002-7863/89/1511-3855$01.50/0

their use as environments for optical studies.[4] In addition, the low thermal conductivity of disordered materials hampers time-dependent studies using laser pulses at low temperatures.[5]

Crystalline materials in general do not have the limitations mentioned above. Inhomogeneous broadening can also occur in crystals as a consequence of imperfections, but, as a rule, low-temperature optical spectra are sharper in crystals than in glasses. Crystals offer the additional advantage of polarization of the incident or emitted light. Furthermore, crystal structure determinations give accurate information of the site symmetry. Luminescence from neat crystals, on the other hand, is often not intrinsic but due to impurities, which act as excitation traps, and great care is therefore necessary in its interpretation. In the family of $4d^6$ and $5d^6$ chelate complexes measurements on neat or diluted crystals have been restricted to only a few examples, $Ru(bpy)_3^{2+}$ (bpy = 2,2'-bipyridine) being the most prominent. Highly resolved optical spectra are very rare indeed.[6-8] Such spectra, in which not only the vibrational side-band structure but also close-lying electronic transitions are individually resolved, are highly valuable complements to low-resolution spectra. They provide the most direct and unambiguous access to spectroscopic parameters such as energy splittings, vibronic coupling, and intensity mechanisms. This information is relevant for an understanding and discussion of the photochemical and photophysical properties of such complexes.

Absorption and emission bands of d^6 metal chelate complexes are generally observed in the visible and ultraviolet regions of the spectrum. These transitions are usually classified as (i) metal-centered (MC) or d-d excitations, (ii) metal-to-ligand charge-transfer (MLCT) or d-π^* excitations, and (iii) ligand-centered (LC) or π-π^* excitations. The nature of the lowest energy excited states is of special interest, since they usually have a much longer life than higher excited states and thus determine the photophysical and photochemical properties. Their classification in terms of the above categories is often possible on the basis of solution spectra, luminescence lifetimes, and electrochemical data. Problems arise when two or more of the above types of excitations are similar in energy. A more specific and detailed study of the relevant states is necessary to determine whether the classification scheme is still valid or whether configurational mixing is important. These crossover situations are of special interest because the excited-state properties are most susceptible to slight physical or chemical variations.

In the title complex the metal ion Rh^{3+} has a $4d^6$ low-spin electron configuration. 2-Phenylpyridine ($phpy^-$), which is isoelectronic with 2,2'-bipyridine (bpy), acts as a chelating ligand with nitrogen and carbon donor atoms. The metal ion is coordinated by six atoms: N_4C_2. N-Rh bond lengths are approximately 2.14 Å for bpy and 2.06 Å for $phpy^-$. The Rh-C bonds are in cis position with 1.99 Å bond lengths.[9] The symmetry group of the complex in solution is $\{C_2\}$. Both ligands exert a strong ligand field, and the lowest energy d-d excitations are expected above 26 000 cm^{-1}, and they have been neglected in the discussion of the first excited states. $[Rh(phpy)_2bpy]^+$ and its Ir^{3+} analogue $[Ir(phpy)_2bpy]^+$ have been prepared and characterized by absorption, luminescence, lifetime, electrochemical, and NMR measurements.[10-15]

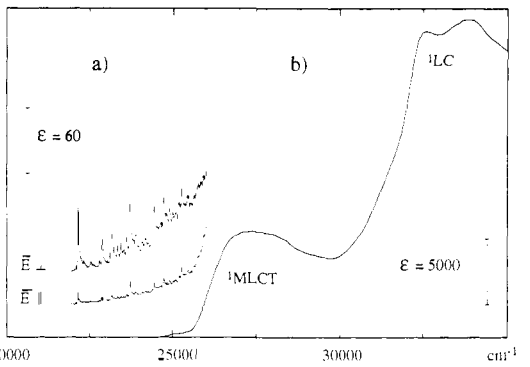

Figure 1. Single-crystal absorption spectrum at 11 K of $[Rh(phpy)_2(bpy)]PF_6$ (a) and absorption spectrum of $[Rh(phpy)_2(bpy)]^+$ in a poly(methyl methacrylate) (PMMA) glass (b). The spectrum is corrected for PMMA absorption. $E_\parallel$ and $E_\perp$ refer to the polarization of the incident beam with respect to the needle axis of the crystal.

In contrast to the corresponding $(bpy)_3$ complexes, in which the emission originates from a state with dominant $^3(\pi-\pi^*)$ character, the situation is much less clear in the mixed-ligand complexes. A MLCT, either to bpy or $phpy^-$ or both, becomes energetically competitive, and the orbital parentage of the emitting state may no longer be pure. For $[Rh(phpy)_2bpy]^+$ an assignment of the first excited state to a ligand-centered triplet on $phpy^-$ was favored, with the possibility of some mixing with a Rh → $phpy^-$ charge-transfer configuration.[11] In $[Ir(phpy)_2bpy]^+$, on the other hand, a dominant Ir → bpy charge-transfer character of the emitting state was postulated.[15] It is clear that more information is needed for a full characterization and understanding of the first excited states in the mixed chelate complexes. There are a variety of physical techniques all of which have been applied to $Ru(bpy)_3^{2+}$, which can provide additional information.[1]

We here report on low-temperature high-resolution spectra of crystalline $[Rh(phpy)_2bpy]PF_6$. This compound can be prepared in the form of single crystals large enough for absorption spectroscopy. Its emission spectrum below 10 K is intrinsic. By a combination of low-temperature absorption and emission spectroscopy, we can improve the picture of the first excited electronic states considerably.

2. Experimental Section

$[Rh(phpy)_2bpy]PF_6$ was synthesized and purified as described in ref 12. Single crystals with dimensions up to 0.1 mm × 0.5 mm × 2 mm were grown from a dichloromethane solution by slow addition of ether. The needlelike crystals showed extinction directions parallel and perpendicular to the needle axis. The same solvent mixture of 4:5 propionitrile/butyronitrile as in ref 11 was used for the luminescence measurements in a glassy matrix. The concentration of the complex in this solution was 6.6×10^{-4} M. Another glassy sample, used for absorption spectra, was prepared by evaporation of a 10% w/v solution of poly(methyl methacrylate) (PMMA, plexiglass) in dichloromethane (complex concentration 2×10^{-4} M). Since the powder of the Cl^- and the PF_6^- salts decomposed after repeated exposition to UV light in the presence of humid air, it was sealed in glass capillaries under low pressure (10^{-3} mbar). These samples did not show any degradation during 1 yr.

Absorption spectra of PMMA films cooled in a closed-cycle helium cryostat (Air Products CSA-202G) were recorded on a Cary 17 spectrophotometer. For all crystal measurements down to 5 K the samples were cooled in a double-walled helium-gas flow tube.[16] A 1402 Spex double monochromator equipped with a Glan-Taylor polarizing prism and a double-beam attachment built in this laboratory was used for the high-resolution absorption spectra. Light of a 100-W halogen lamp was dispersed by two gratings (1200 grooves/mm) blazed at 500 nm, polarized along the extinction directions of the crystal, and detected with an EMI 9781B PM tube. Typical spectral bandwidths were 2.5 cm^{-1}, sufficient to resolve all the sharp features in the spectrum.

For the luminescence measurements sealed glass capillaries containing polycrystalline samples or "nitrile" solution were mounted in the flow tube. A nitrogen laser (PRA LN 250) was used for excitation. The

(4) Krausz, E. R. *J. Lumin.* **1988**, *42*, 283.
(5) Krausz, E. R. *J. Lumin.* **1988**, *42*, 21.
(6) Yersin, H.; Gallhuber, E.; Hensler, G. *Photochemistry and Photophysics of Coordination Compounds*; Springer-Verlag: Berlin, 1987; pp 101-106.
(7) Riesen, H.; Krausz, E.; Puza, M. *Chem. Phys. Lett.* **1988**, *151*, 65.
(8) Komada, Y.; Yamauchi, S.; Hirota, N. *J. Phys. Chem.* **1986**, *90*, 6425.
(9) Mäder, U.; Stöckli, H.; von Zelewsky, A., in preparation.
(10) Mäder, U. Inauguraldissertation, University Fribourg, Switzerland.
(11) Maestri, M.; Sandrini, D.: Balzani, V.; Mäder, U.; von Zelewsky, A. *Inorg. Chem.* **1987**, *26*, 1323.
(12) Mäder, U.; Jenny, T.; von Zelewsky, A. *Helv. Chim. Acta* **1986**, *69*, 1085.
(13) Sandrini, D.; Maestri, M.; Balzani, V.; Mäder, U.; von Zelewsky, A. *Inorg. Chem.* **1988**, *27*, 2640.
(14) Ohsawa, Y.; Sprouse, S.; King, K. A.; De Armond, M. K.; Hanck, K. W.; Watts, R. J. *J. Phys. Chem.* **1987**, *91*, 1047.
(15) King, K. A.; Finlayson, M. F.; Spellane, P. J.; Watts, R. J. *Sci. Pap. Inst. Phys. Chem. Res. (Jpn.)* **1984**, *78*, 97.
(16) Krausz, E. R.; Tomkins, C.; Adler, H. *J. Phys. E* **1982**, *15*, 1167.

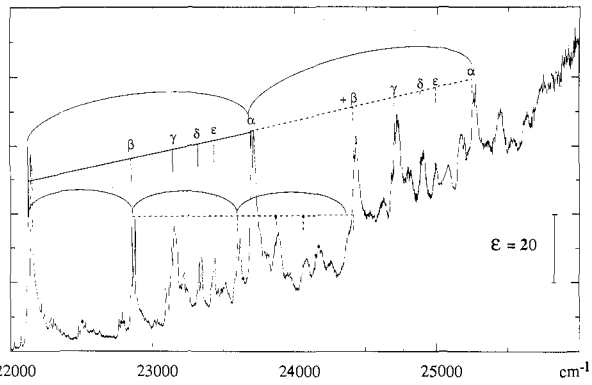

Figure 2. High-resolution polarized ($E_\perp$ needle) crystal absorption spectrum at 11 K of the PF_6^- salt in the region of lowest energy excitations. Progressions and combinations of vibrations account for the sideband structure as indicated.

luminescence was dispersed by the 1402 Spex double monochromator and detected by a cooled RCA 31034 end window photomultiplier and a photon-counting system (Spex DPC-2). All luminescence spectra were corrected for monochromator and PM response. For the excitation spectrum a dye laser (LSI DCM-2) with a stirred 5.7×10^{-3} M solution of Coumarin 120 (Radiant Dyes Chemie) in methanol and pumped by the nitrogen laser was used. A Tektronix 4052A microcomputer was used for monochromator control and data acquisition.

3. Results

Figure 1a shows polarized single-crystal absorption spectra of $[Rh(phpy)_2(bpy)]PF_6$ at 11 K (a) and $[Rh(phpy)_2(bpy)]^+$ in a poly(methyl methacrylate) (PMMA) glass (b) at 14 K. The glass spectrum is in good correspondence with the corresponding 298 K spectrum in a nitrile glass reported in ref 11. The assignment of the intense bands around 27 500 and 33 000 cm^{-1}, respectively, to ^{1}MLCT and ^{1}LC excitations follows from a comparison with the absorption spectra of $Rh(bpy)_3^{3+}$ and phpyH.[11] It is not clear, however, whether only one—and which one—or both of the aromatic chelate ligands are involved in these transitions. The crystal absorption spectrum covers the energy range 22 000–26 000 cm^{-1} between the very lowest excited state of the complex and the intense ^{1}MLCT absorption. The absorption spectrum of the glass at 14 K shows a featureless weak absorption in this region. In contrast, the crystal spectrum exhibits a great deal of fine structure, as shown in detail in Figure 2. The richness and sharpness of this structure is unmatched in the spectroscopy of d^6 complexes with aromatic chelating ligands. All the features in this spectrum can be interpreted as vibrational sidebands on the two prominent origins C and D, as discussed in detail in section 4.

Figure 3 shows a comparison of the low-temperature luminescence spectra of the title complex in three different environments: nitrile glass (a), the Cl^- salt (b), and the PF_6^- salt (c). The glass spectrum is very similar in energy and intensity distribution to the 77 K luminescence spectrum reported in ref 11. The bands are slightly narrower at 20 K. A comparison of three spectra in Figure 3 shows that they all have the same overall intensity distribution. The energy of the highest energy peak is 260 cm^{-1} higher in the PF_6^- than in the Cl^- with the nitrile glass lying in between. The most striking difference is in the fine structure, which, as in absorption, is most pronounced in the PF_6^- salt. Very sharp lines, whose widths are nearly 2 orders of magnitude smaller than in the chloride and glassy samples, dominate the sideband structure up to 1700 cm^{-1} from the origin. The bulk of the PF_6^- luminescence intensity is more or less unstructured, however, as a result of a relatively intense tail extending from each sharp line toward lower energy. A very similar behavior was observed in the luminescence spectra of 1,10-phenanthroline (phen) and $[Rh(phen)_3](BF_4)_3$.[8]

From the observed extreme differences in the line widths of $[Rh(phpy)_2(bpy)]^+$ in different environments, we immediately conclude that these line widths are inhomogeneous. It is interesting to note that the broadening is most pronounced between the PF_6^- crystal and the Cl^- crystal and not, as one might expect, between the crystals on the one hand and the glass on the other. Inhomogeneous line broadening in crystals due to imperfections is a well-documented phenomenon.[17,18] The sharpness of our lines in the PF_6^- salt demonstrates that the information content of a spectrum can be dramatically increased either by a systematic variation of the counterion or by luck.

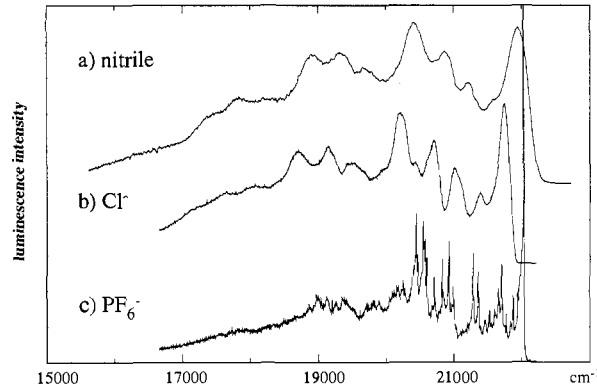

Figure 3. Luminescence spectra of $[Rh(phpy)_2(bpy)]^+$ in three different environments: nitrile glass (a) at 20 K, Cl^- salt (b) and PF_6^- salt (c) at 5 K. The luminescences were excited with the 337-nm line of a nitrogen laser.

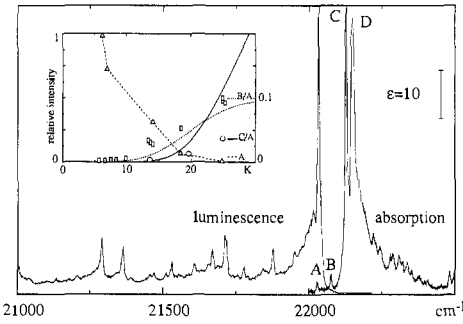

Figure 4. Spectral overlap region of luminescence and absorption spectra at 6 K in the PF_6^- salt. The absorption lines A–D are discussed in the text. The inset shows the temperature dependence of intensity for the transitions B and C in luminescence with the full line corresponding to the calculated Boltzmann populations. Intensities were scaled with the intensity of line A, which decreases with temperature as a result of energy transfer.

Figure 4 shows high-resolution low-temperature absorption and luminescence spectra of the PF_6^- salt in the origin region, where luminescence and absorption spectra overlap. The prominent luminescence origin at 22 030 cm^{-1} coincides with the lowest energy line A in the crystal absorption spectrum; hence, it must be an electronic origin. Lines on the low-energy side of the luminescence origin are transitions to vibrationally excited ground-state levels. The three lines B–D in the absorption spectrum, which are separated from A by 48, 98, and 120 cm^{-1}, respectively, can also be assigned as electronic origins for the following reasons. The very intense absorption lines C and D have no counterparts in the emission spectrum, with the resulting lack of mirror symmetry between absorption and emission about the low-temperature origin A. Lines B and C appear as hot bands in the luminescence spectrum. As shown in the inset of Figure 4, their temperature dependence is approximately as expected for a Boltzmann distribution among three levels separated by 48 and 98 cm^{-1}. It is opposite to what would be expected if the lines A and B were due to trap emission.

The most direct proof that all the four lines are intrinsic is provided by the excitation spectrum as well as the luminescence

(17) Riesen, H.; Güdel, H. U. *Chem. Phys. Lett.* **1987**, *133*, 429.
(18) (a) Thijssen, N. P. N.; Dicker, A. J. M.; Völker, S. *Chem. Phys. Lett.* **1982**, *92*, 7. (b) Wild, U. P.; Lüönd, M.; Meister, E.; Suter, G. W. *J. Lumin.* **1988**, *40 & 41*, 270.

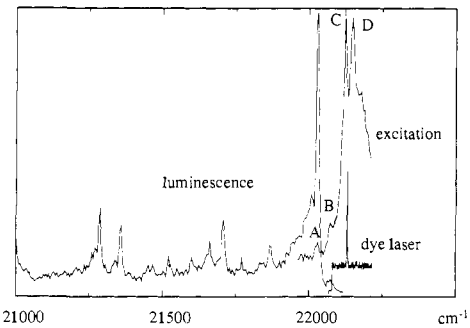

Figure 5. Excitation spectrum of the 5 K luminescence of $[Rh(phpy)_2(bpy)]PF_6$ in the region of the first electronic origins A–D. The luminescence was monitored at 20 500 cm^{-1}. The 5 K luminescence spectrum excited into the C origin is also shown. The output of the dye laser used in these experiments is shown at the bottom with a typical fluorescence background level at $^1/_4$ of the peak output.

Table I. Positions and Intensities of the Four Observed Electronic Origins

line	energy, cm^{-1}	ϵ, M^{-1} cm^{-1}	$f \times 10^8$
A	22 030 + 0	1.7	6.4
B	48	3.8	11
C	98	60	280
D	120	57	500

spectrum obtained by selectively exciting line C. Both are reproduced in Figure 5, which also shows the typical dye laser characteristics. All four lines A–D appear at identical energies and with the same intensity ratios as in the absorption spectrum. The luminescence spectrum with the exciting laser tuned into line C is indistinguishable from the nonselective spectrum using nitrogen laser excitation, which again is in favor of a single chromophor/luminophor spectrum. Additional evidence that the observed properties are intrinsic is provided by luminescence lifetime measurements below 10 K, which give similar values for the PF_6^- salt and the nitrile glass. The relevant properties of the transitions A–D are collected in Table I.

In Figure 6 the vibrational sideband structure of the 11 K absorption and 5 K luminescence spectra can be easily compared. When viewed with low resolution, similarities in the intensity distribution of the sideband structure of the two spectra are readily recognized. On the other hand, the differences in detail, which are brought out by the high resolution, are quite obvious. They will be discussed in detail in section 4.

4. Discussion

The first excited state in $Rh(bpy)_3^{3+}$ has an energy of approximately 22 300 cm^{-1}. Its properties have been studied in detail by optically detected magnetic resonance (ODMR) and luminescence spectroscopy.[8,19] Lifetimes of 2.0 and 3.6 ms have been reported for a nitrile glass[11] and neat $[Rh(bpy)_3]Cl_3$,[8] respectively, at 77 K. This is 2–3 orders of magnitude shorter than τ = 819 ms for bpy in durene.[8] The zero-field splitting of this triplet state, on the other hand, is very similar in $Rh(bpy)_3^{3+}$ and bpy: three levels with a total spread of 0.11 and 0.12 cm^{-1}, respectively.[8] The energetic perturbation of the first ^{3}LC excited state in bpy by coordination to Rh^{3+} is thus minimal, and we can view the lowest energy excitations of the tris complex as localized on individual bpy ligands. A similar conclusion was reached from a study of mixed $[Rh(phen)_m(bpy)_{3-m}]^{3+}$ complexes.[20,21]

Replacing one or two of the bpy ligands by $phpy^-$ in the Rh^{3+} complex will not greatly affect the ^{3}LC transitions on bpy, which we expect around 22 300 cm^{-1}. Whether they will still constitute the lowest excited states is open to question, however, because there are four contenders now in the mixed chelate complex: (i) ^{3}LC transitions on bpy, (ii) ^{3}LC transitions on $phpy^-$, (iii) Rh → bpy ^{3}MLCT, and (iv) Rh → $phpy^-$ ^{3}MLCT transitions. (iii) and (iv) become competitive because of the σ electron donor properties of $phpy^-$. For the present discussion, it is justified to adopt the view of Crosby et al. reached from a comparative study of the mixed chelate complexes $[Ru(phen)_m(bpy)_{3-m}]^{2+}$ that it may not be meaningful to distinguish between (iii) and (iv), i.e. localized descriptions of charge-transfer processes.[21] For a more detailed analysis of the electronic origin region, the different chemical nature of the ligands will have to be considered.[7] The broad absorption band in $[Rh(phpy)_2bpy]^+$ centered at 27 500 cm^{-1} (Figure 1) is undoubtedly a charge-transfer transition, and since we have no evidence of more than one transition, this view is an acceptable starting point for our discussion. The 27 500-cm^{-1} band is a spin-allowed ^{1}(RhLCT) transition, and we can estimate the expected position of the corresponding ^{3}(RhLCT) states from a comparison with $Ru(bpy)_3^{2+}$. The difference between the lowest energy absorption band and the center of the ^{1}(RuLCT) absorption in $Ru(bpy)_3^{2+}$ is about 4000 cm^{-1}.[22]

We thus expect the onset of the ^{3}(RhLCT) absorptions below 24 000 cm^{-1}. Due to their MLCT character, i.e. participation of a heavy metal, these absorptions are expected to have oscillator strengths, which are 2–3 orders of magnitude higher than those for the ligand-centered ^{3}LC transitions. They should therefore dominate the absorption spectrum below 26 000 cm^{-1}.

On this basis, there is only one plausible assignment for the highly structured absorption band observed in crystals of $[Rh(phpy)_2bpy]PF_6$ between 22 000 and 26 000 cm^{-1} (Figures 1 and 2): ^{3}(RhLCT) transitions.

We now turn to a discussion of the sideband structure and its implications. The assignment of the vibrational sidebands in the crystal absorption spectrum is indicated in Figure 2. From the fact that the intensity ratio of the $E_\perp$ and $E_\parallel$ polarized crystal spectra is approximately 4.4 over the whole range of highly structured absorption bands (Figure 1), we can draw the following conclusions: (i) the electronic transitions have pronounced molecular polarizations, i.e. their transition moments are anisotropic; (ii) the two transitions with origins C and D have the same molecular polarization, and it is thus very likely that the states C and D have the same physical nature; (iii) all of the sideband intensity is totally symmetric. By a combination of only five vibrations, designated α–ϵ in Figure 2, all the major sidebands can be interpreted. For the 1569 cm^{-1} (α) and 730 cm^{-1} (β) vibrations, the first three members of a progression can be clearly identified and determined. The α vibration dominates the sideband structure, occurring in combination with all the other vibrations. From the intensity distribution in the two resolved progressions, we can determine Huang–Rhys factors, which are defined as[23]

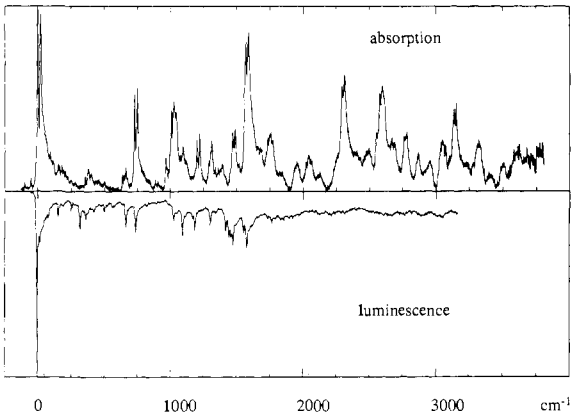

Figure 6. 11 K absorption and 5 K luminescence spectra of the PF_6^- salt on the same energy scale. From the measured absorption spectrum (Figure 2) the rising broad background was subtracted. The origin of luminescence was lined up with the origin C in absorption.

(19) van Oort, E.; Sitters, R.; Scheijde, J. H.; Glasbeek, M. *J. Chem. Phys.* **1987**, *87*, 2394.
(20) Halper, W.; DeArmond, M. K. *J. Lumin.* **1972**, *5*, 225.
(21) Crosby, G. A.; Elfring, W. H. *J. Phys. Chem.* **1976**, *80*, 2206.
(22) Felix, F.; Ferguson, J.; Güdel, H. U.; Ludi, A. *Chem. Phys. Lett.* **1979**, *62*, 153.

$$S_i = n\frac{I_n}{I_{n-1}} \quad (1)$$

where i designates the mode and I_n the dipole strength of the nth line in the progression. We obtain $S_\alpha = 1.1 \pm 0.1$ and $S_\beta = 0.7 \pm 0.1$. These values are in good agreement with a charge-transfer assignment. In $Ru(bpy)_3^{2+}$ a rough estimate of the Huang–Rhys factor in the 1380-cm^{-1} mode, which dominates the luminescence spectrum, is $S = 1.0$, very similar to our corresponding S_α value.[1,24] In $Ru(bpy)_3^{2+}$ the luminescent states are considered to have predominant MLCT character. Huang–Rhys factors are a measure of the displacement of excited-state potential surfaces with respect to certain molecular coordinates. The highly resolved crystal absorption spectrum of $[Rh(phpy)_2bpy]PF_6$ allows a determination of individual Huang–Rhys factors. The two numbers for S_α and S_β given above indicate that the displacements along the two coordinates are different.

There are some notable differences between the behavior of the lowest energy absorptions in $[Rh(phpy)_2(bpy)]^+$ and $[Ru(bpy)_3]^{2+}$. In our complex the origins (C and D) are prominent, whereas in $[Ru(bpy)_3]^{2+}$, they are negligibly weak and most of the ^{3}MLCT absorption (and emission) intensity appears to be vibronically induced.[1] The loss of trigonal symmetry in our mixed chelate complex with two ligands of very different electron donor properties leads to a strong electric dipole moment in the Rh–bpy direction. It is therefore intuitively understandable that also the RhLCT transition dipole moment has a large component in this direction.

Having identified the transitions C and D (including their sideband structure) as predominantly ^{3}(RhLCT) in origin, we now concentrate on the transitions A and B. From Figure 3 we see that the overall intensity distribution in the low-temperature luminescence spectrum of $[Rh(phpy)_2(bpy)]^+$ is roughly the same for all the samples. We do not see any major changes in intensity distribution with temperature up to 100 K in the nitrile glass spectrum. From the poorly resolved Cl^- and nitrile spectra in Figure 3 we estimate a Huang–Rhys factor $S = 1.4 \pm 0.3$ for the progression in the 1550-cm^{-1} mode. This has to be compared with $S_\alpha = 1.1 \pm 0.1$ derived for the C and D transitions in absorption. We conclude that overall Huang–Rhys factors based on low-resolution spectra do not allow a discrimination between the transition A and the transitions C and D.

The differences become evident in the highly resolved crystal spectra of the PF_6^- salt, and the representation in Figure 6 is best suited for a comparative discussion. The emission spectrum is highly resolved up to 1700 cm^{-1}, with a much larger number of prominent individual sidebands than in the absorption spectrum. Above 1700 cm^{-1} the structure is washed out in the emission spectrum as a result of the high density of states and the low-energy tail associated with each band. In contrast, the absorption spectrum shows well-resolved combination bands out to 3500 cm^{-1}, and this despite the fact that it is superimposed by the rising background between 23 000 and 26 000 cm^{-1}. Another significant difference in the sideband structure is in the low-energy region up to 730 cm^{-1}. There are no major sidebands in this region in absorption, whereas the emission spectrum shows several lines that are comparable in intensity with the higher energy sidebands.

These differences in the sideband structure between absorption and luminescence are significant. They indicate a selectivity for certain modes in the absorption process, which does not operate in emission. The transitions to the ^{3}(RhLCT) states C and D, which dominate the low-energy crystal absorption spectrum, must be of a different nature to the luminescence transition from the state A. It is therefore tempting to assign A and B, and thus the low-temperature luminescence spectrum, to ligand-centered ^{3}LC transitions. Such an assignment has various attractions. Besides the differences between the low-temperature absorption and emission spectra, the disparity in intensity between the lines A,B and C,D is partly explained. In addition, the position of the lines A and B is very close to the expected energy of the lowest bpy and $phpy^-$ centered ^{3}LC electronic origins. But there are some observations that are hard to reconcile with a pure ^{3}LC assignment for the bands A and B. The luminescence decay rate is about 1 order of magnitude too high. We measure a value $\tau^{-1} = 5960$ s^{-1} at 77 K in the nitrile glass, compared to $\tau^{-1} = 500$ s^{-1} at 77 K for $Rh(bpy)_3^{3+}$.[11] The splitting of the two lines A and B of 48 cm^{-1} is 2 orders of magnitude larger than the splitting of 0.12 cm^{-1} in the first triplet state of $Rh(bpy)_3^{3+}$.[8] It is thus not likely to be a zero-field splitting in the usual sense. On the other hand, preliminary measurements of the magnetic circularly polarized luminescence (MCPL) indicate that the first level A does not have the typical properties of a ligand-centered triplet state.[25]

It appears therefore that in some respects the excited states A and B behave like ligand-centered $^3(\pi-\pi^*)$ states and in some respects they do not. This can be rationalized by the proximity of the states C and D, which have ^{3}(RhLCT) charge-transfer characteristics. The singlet–triplet charge-transfer transitions are orders of magnitude more intense than ligand-centered singlet–triplet excitations. The intensity and thus the decay rate of the latter will be strongly affected by a possible mixing of $\pi-\pi^*$ and (RhLCT) electron configurations. The properties of the charge-transfer transitions, on the other hand, will not be strongly affected by mixing in some $^3(\pi-\pi^*)$ character. An additional effect is expected from the increased covalency of the Rh–C($phpy^-$) bonds compared to the Rh–N bonds. This will result in a stronger Rh character of the π^* "ligand" orbitals than in $Rh(bpy)_3^{3+}$.

High-resolution optical spectroscopy of crystalline samples proves to be a very powerful tool for elucidating the nature of the first excited states in the title complex. A number of questions, particularly concerning the transitions A and B, have no definite answer yet. We are therefore extending our experimental study, and one of our primary aims is a determination of the magnetic properties of the first excited states. Another aspect of interest is theoretical: the detailed experimental picture should provide a sufficient basis for a more detailed investigation of the "mixing" between charge-transfer and ligand-centered excitations.

Acknowledgment. We thank Ch. Reber and E. R. Krausz for many useful discussions. This work was financially supported by the Swiss National Science Foundation.

(23) (a) Wilson, R. B.; Solomon, E. I. *J. Am. Chem. Soc.* **1980**, *102*, 4085. (b) Yersin, H.; Otto, H.; Zink, J. I.; Gliemann, G. *J. Am. Chem. Soc.* **1980**, *102*, 951.

(24) Caspar, J. V.; Meyer, T. J. *J. Am. Chem. Soc.* **1983**, *105*, 5583.

(25) Zilian, A.; Güdel, H. U., unpublished results.